Hindawi
Discrete Dynamics in Nature and Society
Volume 2023, Article ID 8840525, 13 pages
https://doi.org/10.1155/2023/8840525

Research Article

Behind Jarratt's Steps: Is Jarratt's Scheme the Best Version of Itself?

Alicia Cordero,[1] **Elaine Segura**,[2] **and Juan R. Torregrosa**[1]

[1]*Instituto Universitario de Matemática Multidisciplinar, Universitat Politècnica de València, Valencia, Spain*
[2]*Departamento de Matemática, Universidad Autónoma de Santo Domingo, Santo Domingo, Dominican Republic*

Correspondence should be addressed to Juan R. Torregrosa; jrtorre@mat.upv.es

Received 9 March 2023; Revised 8 May 2023; Accepted 26 May 2023; Published 15 June 2023

Academic Editor: Abdellatif Ben Makhlouf

In this paper, we analyze the stability of the family of iterative methods designed by Jarratt using complex dynamics tools. This allows us to conclude whether the scheme known as Jarratt's method is the most stable among all the elements of the family. We deduce that classical Jarratt's scheme is not the only stable element of the family. We also obtain information about the members of the class with chaotical behavior. Some numerical results are presented for confirming the convergence and stability results.

1. Introduction

The solution of nonlinear equations and systems of equations is among the most important problems, both from a theoretical and a practical point of view, in applied mathematics and other sciences, see for example [1]. Due to the lack of analytical methods for solving such problems, iterative methods are becoming increasingly necessary for approximating the solutions of these equations.

In addition to the classical methods such as Newton, Chebyshev, and Halley among the so-called one-point methods, and multipoint algorithms such as Traub, Jarratt, and Ostrowski, numerous papers have been published in recent years trying to overcome the convergence order of these schemes as well as their stability. In all of them, the authors construct iterative procedures for approximating simple roots α of a nonlinear equation $f(x) = 0$, where $f: I \subseteq \mathbb{R} \longrightarrow \mathbb{R}$ is a real function defined on an open interval I. In the books [2, 3], we can found good overviews of this area of numerical analysis.

The dynamical analysis of an iterative method or a family of schemes is a valuable tool for classifying the different iterative formulas, not only in terms of their order of convergence but also in terms of their behavior in terms of the chosen of initial guesses. This study also provides useful information on the stability and reliability of the iterative methods. See, for example, [4–6].

In this paper, we present a dynamical study of the parametric Jarratt family, a set of fourth-order iterative methods for approximating simple roots α of a nonlinear equation $f(x) = 0$. In [7], Jarratt designed a fourth-order formula for solving nonlinear equations which require three functional evaluations per iteration, one of f and two of f'. Its expression is as follows:

$$x_{k+1} = x_k - \phi_1(x_k) - \phi_2(x_k), \tag{1}$$

where

$$\begin{aligned} \phi_1(x_k) &= a_1 w_1(x) + a_2 w_2(x), \\ \phi_2(x_k) &= \frac{f(x)}{b_1 f'(x) + b_2 f'[x + \gamma w_1(x)]}, \end{aligned} \tag{2}$$

being

$$\begin{aligned} w_1(x) &= \frac{f(x_k)}{f'(x_k)}, \\ w_2(x) &= \frac{f(x_k)}{f'[x_k + \gamma w_1(x)]}, \end{aligned} \tag{3}$$

and a_1, a_2, b_1, b_2, and γ real or complex parameters.

Using Taylor's series expansion around a simple zero α of $f(x) = 0$, Jarratt obtained values of some of the previous parameters to reach fourth-order convergence. Taking $\theta = b_2/b_1 + b_2$ and $\gamma = -2/3$ and expressing Jarratt's class in two steps, we obtain

$$\begin{cases} y_k = x_k - \dfrac{2}{3}\dfrac{f(x_k)}{f'(x_k)}, \\ \\ x_{k+1} = x_k - \left(\dfrac{2\theta - 3}{8\theta}\right) w_1(x) - \left[\dfrac{6\theta - 9}{8(\theta - 1)}\right] w_2(x) - \dfrac{\theta f(x_k)}{b_2(1-\theta)f'(x_k) + \theta b_2 f'(y_k)}, \end{cases} \tag{4}$$

where $w_1(x_k) = f(x_k)/f'(x_k)$, $w_2(x_k) = f(x_k)/f'(y_k)$, $k = 0, 1, 2, \ldots$, $b_2 = 8\theta^2/3(\theta - 1)$, and θ is an arbitrary parameter that can take real or complex values. $\theta \neq 0, 1$, otherwise the method is not defined. This parametric family includes the so-called Jarratt's method, for $\theta = 3/2$, whose iterative expression is as follows:

$$\begin{cases} y_k = x_k - \dfrac{2}{3}\dfrac{f(x_k)}{f'(x_k)}, \\ \\ x_{k+1} = x_k - \dfrac{1}{2}\dfrac{3f'(y_k) + f'(x_k)}{3f'(y_k) - f'(x_k)}\dfrac{f(x_k)}{f'(x_k)}. \end{cases} \tag{5}$$

1.1. Dynamical Concepts. We are going to analyze the stability of members of family (4). For it, we apply complex dynamics tools to the rational operator obtained when this class is applied on an arbitrary second degree polynomial $p(x)$. We recall some concepts of complex dynamics that we use in this work. For a more general understanding of these concepts, see, for example, [8, 9].

Given a rational operator $R: \widehat{\mathbb{C}} \longrightarrow \widehat{\mathbb{C}}$ defined on the Riemann sphere, $\widehat{\mathbb{C}}$, the orbit of a point x_0 is the sequence of points.

$$\{x_0, R(x_0), R^2(x_0), \ldots, R^n(x_0), \ldots\}. \tag{6}$$

A fixed point x_0 of operator R is a point such that $R(x_0) = x_0$. If a fixed point is not a root of polynomial $p(x)$, then it is called a strange fixed point. Fixed points can be classified according to the behavior of the derivative operator on them. Therefore, a fixed point x_0 is an attracting point if $|R'(x_0)| < 1$, superattracting if $|R'(x_0)| = 0$, repulsing if $|R'(x_0)| > 1$ and parabolic or neutral if $|R'(x_0)| = 1$.

A critical point of operator R is a point x_0 where the derivative of R cancels out, that is, $R'(x_0) = 0$. Critical points that do not coincide with the roots of the polynomial are called free critical points.

The basin of attraction of an attractor α is defined as the set of preimages of any order that satisfy the following equation:

$$A(\alpha) = \{x_0 \in \widehat{\mathbb{C}}: R^n(x_0) \longrightarrow \alpha, n \longrightarrow \infty\}. \tag{7}$$

The rest of the paper is organized as follows. In Section 2, the convergence order of the parametric family (4) is analyzed. The dynamical behavior of this family as a function of parameter θ is studied in Section 3. First, we determine the rational operator associated with the family and analyze the stability of the corresponding fixed points and critical points of that operator. The parameter planes of the free critical points are drawning, which allows visualizing the parameter values that make the method stable or unstable. Finally, the dynamical planes are generated, in which the basins of attraction of fixed or periodic points of the method can be visualized for some particular value of the parameter. In Section 4, some numerical tests are presented to compare the family of methods studied with other schemes. The paper ends with some conclusions, which are presented in Section 5 along with the references used.

2. Convergence of Jarratt Parametric Family

In this section, the convergence analysis of the Jarratt parametric family is studied. We present an alternative proof to that given by Jarratt. From the error equation, we can observe that all the members of uniparametric family (4) have fourth-order convergence, with independence of parameter θ.

Theorem 1. *Let $f: I \subset \mathbb{R} \longrightarrow \mathbb{R}$ be a sufficiently differentiable function at each point of the open interval I such that $\alpha \in I$ is a simple root of $f(x) = 0$. If we choose an initial estimate x_0 sufficiently close to α, sequence $\{x_k\}_{k \geq 0}$ obtained using iterative expression (4), converges to α, with order of convergence $p = 4$, being the error equation.*

$$e_{k+1} = \frac{1}{9}\left((21 - 8\theta)C_2^3 - 9C_2C_3 + C_4\right)e_k^4 + O\left(e_k^5\right), \tag{8}$$

where $C_j = 1/j!f^{(j)}(\alpha)/f'(\alpha)$, $j = 2, 3, \ldots$ *y* $e_k = x_k - \alpha$, $\forall k \in \mathbb{N}$.

Proof. Using Taylor's series expansion of the function $f(x_k)$ and $f'(x_k)$ around α, we have

$$f(x_k) = f'(\alpha)e_k + f'(\alpha)C_2e_k^2 + f'(\alpha)C_3e_k^3 + f'(\alpha)C_4e_k^4 + O\left(e_k^5\right), \tag{9}$$

$$f'(x_k) = 2f'(\alpha)C_2e_k + 3f'(\alpha)C_3e_k^2 + 4f'(\alpha)C_4e_k^3 + O\left(e_k^4\right). \tag{10}$$

Calculating the quotient $w_1(x_k) = f(x_k)/f'(x_k)$,

$$w_1(x_k) = e_k - C_2e_k^2 + \left(2C_2^2 - 2C_3\right)e_k^3 + \left(-4C_2^3 + 7C_2C_3 - 3C_4\right)e_k^4 + O\left(e_k^5\right). \tag{11}$$

From the equations (3)–(5) and the first step of the iterative scheme (4), we have

$$y_k - \alpha = \frac{e_k}{3} + \frac{2C_2e_k^2}{3} - \frac{4}{3}\left(C_2^2 - C_3\right)e_k^3 + \frac{2}{3}\left(4C_2^3 - 7C_2C_3 + 3C_4\right)e_k^4 + O\left(e_k^5\right). \tag{12}$$

The Taylor's series expansion of $f(y_k)$ is as follows:

$$\begin{aligned} f(y_k) = {} & \frac{f'(\alpha)e_k}{3} + \frac{7}{9}f'(\alpha)C_2e_k^2 + \left(-\frac{8}{9}f'(\alpha)C_2^2 + \frac{37f'(\alpha)C_3}{27}\right)e_k^3 \\ & + \frac{1}{81}f'(\alpha)\left(180C_2^3 - 288C_2C_3 + 163C_4\right)e^4 + O\left(e^5\right), \end{aligned} \tag{13}$$

and the derivative of function $f(y_k)$ is as follows:

$$f'(y_k) = f'(\alpha) + \frac{2}{3}f'(\alpha)C_2e_k + \frac{1}{3}f'(\alpha)\left(4C_2^2 + C_3\right)e_k^2 + \frac{4}{27}f'(\alpha)\left(-18C_2^3 + 27C_2C_3 + C_4\right)e_k^3 + O\left(e_k^4\right). \tag{14}$$

Calculating the quotient $w_2(x_k) = f(x_k)/f'(y_k)$,

$$w_2(x_k) = e_k + \frac{C_2e_k^2}{3} + \left(-\frac{14C_2^2}{9} + \frac{2C_3}{3}\right)e_k^3 + \left(\frac{112C_2^3}{27} + C_2\left(-\frac{8C_2^2}{9} - \frac{C_3}{3}\right) - \frac{38C_2C_3}{9} + \frac{23C_4}{27}\right)e_k^4 + O\left(e_k^5\right). \tag{15}$$

Substituting equations (11) and (15) in the second step of the iterative expression (4) yields error equation for Jarratt parametric family as follows:

$$e_{k+1} = \frac{1}{9}\left((21 - 8\theta)C_2^3 - 9C_2C_3 + C_4\right)e_k^4 + O\left(e_k^5\right). \tag{16}$$

This completes the proof.

According to Kung and Traub's conjecture (see [10]), the family shown in (4) is optimal. □

3. Complex Dynamical Behavior

In this section, we present a dynamical study of Jarratt's family (4). We begin by calculating the rational operator

associated with the class when it is applied on a quadratic polynomial and then analyze the stability of the fixed and critical points of this operator. From the independent critical points, we generate the parameter spaces, which are graphs that allow us to visually determine the values of the parameter for which a member of the family has stable or unstable behavior.

3.1. Rational Operator. We analyze family (4) on a generic quadratic polynomial $p(x) = (x-a)(x-b)$, with zeros $a, b \in \mathbb{C}$. The result is a rational operator, called K, which depends on a, b, and parameter θ:

$$K_{p,\theta}(x) = x - \frac{(-a+x)(-b+x)(1+3/2\theta)}{4(-a-b+2x)} - \frac{(-a+x)(-b+x)}{8/3(-a-b+2x)(1-\theta)(-1+\theta)\theta + 8/3(-a-b+2(x-(2(-a+x)(-b+x))/(3(-a-b+2x))))(-1+\theta)\theta^2} - \frac{3(-a+x)(-b+x)(1-1/(-2+2\theta))}{4(-a-b+2(x-(2(-a+x)(-b+x))/(3(-a-b+2x))))}. \tag{17}$$

Proposition 2. *Let $p(x) = (x-a)(x-b)$ be a generic quadratic polynomial, with zeros $a, b \in \mathbb{C}$. The rational function associated to the Jarratt parametric family, after applying Möbius transformation, is as follows:*

$$R_\theta(x) = \frac{x^4(-21 - 3x(8+3x-4\theta) + 8\theta)}{-9 - 3x(8+7x) + 4x(3+2x)\theta}, \tag{18}$$

where $\theta \in \mathbb{C}$ is an arbitrary parameter. Moreover, if $\theta \in \{-3/2, 3/2, 27/10\}$, the operator is simplified as follows:

$$R_{-3/2}(x) = \frac{x^4(11+3x)}{3+11x}, \tag{19}$$

$$R_{3/2}(x) = x^4, \tag{20}$$

$$R_{27/10}(x) = -\frac{x^4(1+15x)}{15+x}. \tag{21}$$

For $\theta = 3/2$, we can observe that Cayley's test is satisfied.

Proof. Let $p(x) = (x-a)(x-b)$ be a generic quadratic polynomial, with roots $a, b \in \mathbb{C}$. Applying the iterative scheme given in equation (4) on $p(x)$ we obtain the rational function $K_{p,\theta}(x)$, which depends on roots a, b, and parameter $\theta \in \mathbb{C}$. Using Möbius transformation on $K_{p,\theta}(x)$, with

$$h(x) = \frac{x-a}{x-a}, \tag{22}$$

that satisfies, $h(a) = 0$, $h(b) = \infty$, we obtain (18).

$$R_\theta(x) = \frac{x^4(-21 - 3x(8+3x-4\theta) + 8\theta)}{-9 - 3x(8+7x) + 4x(3+2x)\theta}, \tag{23}$$

which only depends on the arbitrary parameter $\theta \in \mathbb{C}$.

By factoring the numerator and denominator in (18), it can be proved that for $\theta \in \{-3/2, 3/2, 27/10\}$ and the operator $R_\theta(x)$ is simplified as seen in equations (19)–(21), which completes the proof. □

3.2. Fixed Point Analysis. Solving the equation $R_\theta(x) = x$, we obtain the fixed points of operator R_θ.

Proposition 3. *The fixed points of the rational function R_θ are $x = 0$ and $x = \infty$, which correspond with the roots of $p(x)$, and the following are strange fixed points:*

(i) $ex_1 = 1$, *for* $\theta \neq 27/10$,

(ii) $ex_{2,3} = A - B \mp 1/2\sqrt{C-D}$,

(iii) $ex_{4,5} = A + B \mp 1/2\sqrt{C-D}$, *where*

$$A = \frac{1}{12}(-11+4\theta),$$
$$B = \frac{1}{12}\sqrt{-23-8\theta+16\theta^2},$$
$$C = -2 + \frac{1}{18}(11-4\theta)^2 + \frac{2}{9}(-27+10\theta),$$
$$D = \frac{3\left(-8/3(11-4\theta) - 1/27(11-4\theta)^3 - 8/27(11-4\theta)(-27+10\theta)\right)}{2\sqrt{-23-8\theta+16\theta^2}}. \tag{24}$$

The total number of fixed points of operator $R_\theta(x)$ varies as a function of parameter θ, that is,

(i) If $\theta \in \mathbb{C}$ and $\theta \neq 27/10$, then $R_\theta(x)$ has seven fixed points.

(ii) If $\theta = 27/10$, then $\mathrm{ex}_1 = 1$ is not a fixed point and $R_\theta(x)$ has six fixed points.

Pairs of strange fixed points conjugate to each other satisfy $\mathrm{exi} - 1/\mathrm{exj} = 0$ for $i \neq j$; these are ex_2 and ex_3, ex_4, and ex_5.

According to Proposition 3, there are at most seven and at least six fixed points for the rational operator $R_\theta(x)$. In addition, we show the existence of two pairs of strange fixed points conjugate to each other, each pair has the same stability characteristics, and thus, the stability analysis is reduced by half.

3.3. Stability of Fixed Points. In order to analyze the stability of the fixed points, we calculate the first derivative of operator $R_\theta(x)$.

$$R'_\theta(x) = \frac{4x^3\left(27\left((1+x)^2(7+x(10+7x)) - 12\left(6+x\left(62+39x+6x^2\right)\right)\right)\theta + 8x(9+x(22+9x))\theta^2\right)}{(-9-3x(8+7x)+4x(3+2x)\theta)^2}. \tag{25}$$

It is known that 0 and ∞ are superattracting fixed points, since the methods have order of convergence four, regardless of the value of the parameter θ; however, the stability of the strange fixed points depends on the value of θ. The stability of strange fixed points ex_1 to ex_5 is established in the following theorems.

Theorem 4 (Stability of ex_1).

The character of the strange point $ex_1 = 1$, for $\theta \neq 27/10$ is

(i) If $|\theta - 467/154| < 8/77$, *then ex_1 is attracting, and it is a superattracting if $\theta = 3$.*

(ii) If $|\theta - 467/154| = 8/77$, *then ex_1 is a parabolic point.*

(iii) If $|\theta - 467/154| > 8/77$, then ex_1 is repulsing.

Proof. From equation (16), we have

$$R'_\theta(1) = \frac{32(-3+\theta)}{-27+10\theta}. \tag{26}$$

Then,

$|32(-3+\theta)/-27+10\theta| \leq 1 \Leftrightarrow |32(-3+\theta)| \leq |-27+10\theta|$.

Let $\theta = a + \mathrm{bi}$ be an arbitrary complex number. Then,

$$32^2\left(9 - 6a + a^2 + b^2\right) \leq 729 - 540a + 100a^2 + 100b^2. \tag{27}$$

Simplifying, we have

$$924a^2 + 924b^2 - 5604a + 8487 \leq 0. \tag{28}$$

Thus,

$$\left(a - \frac{467}{154}\right)^2 + b^2 \leq \frac{64}{5929}. \tag{29}$$

Therefore,

$$\left|R'_\theta(1)\right| \leq 1 \Longleftrightarrow \left|\theta - \frac{467}{154}\right| \leq \frac{8}{77}. \tag{30}$$

In addition, if θ satisfies $|\theta - 467/154| > 8/77$, then $|R'_\theta(1)| > 1$, ex_1 is repulsing and the proof is finished.

The following results can be demonstrated numerically using the stability functions associated with fixed points. □

Theorem 5 (Stability of ex_2 and ex_3).

The stability of strange fixed points ex_2 and ex_3, for real values of θ, can be summarized as follows:

(i) If $\theta \in -1.0369, 1/4 - \sqrt{6}/2\lceil \cup \mathrm{D}$, where D is the region of the cone below the cardioid in Figure 1, then ex_2 and ex_3 are attractors; if $\theta \approx -0.994035$, they are superattractors.

(ii) If $\theta \in \{1/4 \pm \sqrt{6}/2\} \cup \mathrm{F}$, where F is the boundary of the disk in the region marked in blue in Figure 1, then ex_2 and ex_3 are parabolic points.

(iii) If $\lceil \theta \in -\infty, -1.0369$, then ex_2 and ex_3 are repulsors.

Theorem 6 (Stability of ex_4 y ex_5).

Stability analysis of strange fixed points ex_4 and ex_5, for real values of θ, satisfies the following statements:

(i) If $\theta \in 69/22, 3.33 \cup D$, where D is the region of the cone below the cardioid in Figure 2, then ex_4 and ex_5 are attractors; if $\theta \approx 1.47521$ or $\theta \approx 3.23311$ they are superattractors.

(ii) If $\theta \in \{1/4 \pm \sqrt{6}/2\} \cup \{69/22\} \cup F$, where F is the boundary of the disk in the region marked in blue in Figure 2, then ex_4 and ex_5 are parabolic points.

(iii) If $\theta \in -3/2, 1/4 - \sqrt{6}/2$, then ex_4 and ex_5 are repulsors.

The stability surface of strange fixed point $ex_1 = 1$ in the complex plane can be seen in Figure 3. In it, the zones of attraction (blue surface) and repulsion (gray surface) are shown. Visually, if θ is inside the circumference of the cone, then it is attracting; if θ is on the circumference, it is parabolic and if θ is outside the circumference, it is repulsor.

The stability surface of strange fixed points ex_2 and ex_3 is shown in Figure 1. The stability surface of strange fixed points ex_4 and ex_5 is shown in Figure 2. In these figures, the prevalence of repulsion zones over attraction zones is observed.

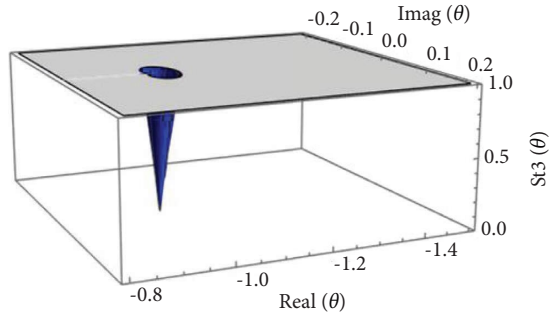

FIGURE 1: Stability surface of ex_2 and ex_3.

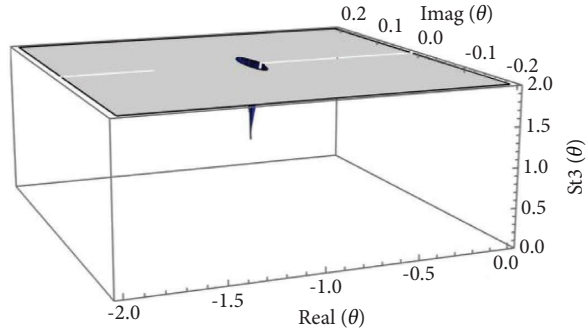

FIGURE 2: Stability surface of ex_4 and ex_5.

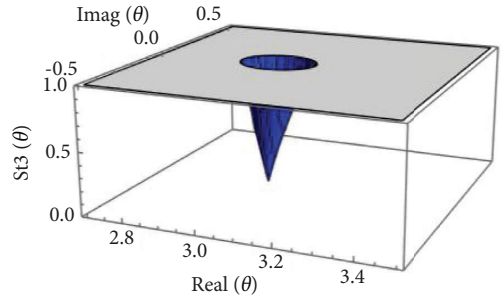

FIGURE 3: Stability surface of $ex_1 = 1$ (in blue, the complex region where the point is an attractor, and in gray the surface where it is a repulsor or parabolic).

3.4. Analysis of Critical Points. We will calculate the critical points of the rational operator $R_\theta(x)$ given in equation (18).

Fatou and Julia [11, 12] stated that these points are of special interest, since each basin of attraction has at least one critical point, so the free critical points could be in a basin of attraction of some of the solutions of the equation, or be in the basin of some strange fixed point or attracting periodic orbit.

Proposition 7. *The critical points of operator $R_\theta(x)$ are the roots of equation $R'_\theta(x) = 0$, that is, $x = 0$ and $x = \infty$ and four free critical points depending on parameter θ:*

(i) $cl_{1,2}(\theta) = E - F\mp\sqrt{2}/3\sqrt{G(-54(-H) + \theta(8397 + I + \theta J))}$,

(ii) $cl_{3,4}(\theta) = E + F\mp\sqrt{2}/3\sqrt{G(54(H) + \theta(8397 - I + K))}$, *where*

$$E = \frac{(-2+\theta)(-9+2\theta)}{-21+8\theta}, F = \frac{\sqrt{81+\theta(18+\theta(45+4\theta(-29+9\theta)))}}{3(21-8\theta)},$$

$$G = \frac{1}{(-21+8\theta)^3},$$

$$H = 189 + (21-8\theta)\sqrt{81+\theta(18+\theta(45+4\theta(-29+9\theta)))}, \tag{31}$$

$$I = 39(21-8\theta)\sqrt{81+\theta(18+\theta(45+4\theta(-29+9\theta)))},$$

$$J = \theta(4\theta(3171+\theta(-773+72\theta)) - 3(7293+2(21-8\theta)\sqrt{81+\theta(18+\theta(45+4\theta(-29+9\theta)))})),$$

$$K = \theta(-21879+4\theta(3171+\theta(-773+72\theta)) + 6(21-8\theta)\sqrt{81+\theta(18+\theta(45+4\theta(-29+9\theta)))}).$$

The total number of different critical points of operator $R_\theta(x)$ varies as a function of parameter θ:

(i) If $\theta \in \mathbb{C}$ and $\theta \notin \{-3/2, 3/2, 27/10\}$, then operator $R_\theta(x)$ has six critical points

(ii) If $\theta = 3/2$, then operator $R_\theta(x)$ simplifies and has two critical points

(iii) If $\theta \in \{-3/2, 27/10\}$, then operator $R_\theta(x)$ simplifies and has four critical points

Pairs of free critical points conjugate to each other satisfy $cl_i = 1/cl_j$; for $i \neq j$; these are: $\mathrm{cl}_1(\theta)$ and $\mathrm{cl}_2(\theta)$, $\mathrm{cl}_3(\theta)$ and $\mathrm{cl}_4(\theta)$. This means that there are only two independent free critical points.

(i) The free critical points $\mathrm{cl}_1(\theta)$ and $\mathrm{cl}_2(\theta)$ coincide for $\theta = 0$,

(ii) The free critical points $\mathrm{cl}_1(\theta)$ and $\mathrm{cl}_3(\theta)$ coincide for the following values of parameter θ:

$$\theta = \frac{3}{2},$$

$$\theta = \frac{1}{54}(31+L+M),$$

$$\theta = \frac{31}{54} - \frac{1}{108}(1+i\sqrt{3})L - \frac{1}{108}(1-i\sqrt{3})M, \tag{32}$$

$$\theta = \frac{31}{54} - \frac{1}{108}(1-i\sqrt{3})L - \frac{1}{108}(1+i\sqrt{3})M.$$

(iii) where

$$L = (208153 - 1296\sqrt{18951})^{1/3},$$
$$M = (208153 + 1296\sqrt{18951})^{1/3}. \tag{33}$$

(iv) The free critical points $\mathrm{cl}_2(\theta)$ and $\mathrm{cl}_4(\theta)$ coincide for the following values of parameter θ:

$$\theta = \frac{3}{2},$$

$$\theta = \frac{1}{54}(31+L+M),$$

$$\theta = \frac{31}{54} - \frac{1}{108}(1+i\sqrt{3})L - \frac{1}{108}(1-i\sqrt{3})M, \tag{34}$$

$$\theta = \frac{31}{54} - \frac{1}{108}(1-i\sqrt{3})L - \frac{1}{108}(1+i\sqrt{3})M.$$

(v) The free critical points $\mathrm{cl}_3(\theta)$ and $\mathrm{cl}_4(\theta)$ coincide for the following values of parameter θ:

$$\theta = -\frac{3}{2},$$

$$\theta = \frac{27}{10}; \tag{35}$$

$$\theta = 3.$$

Proposition 7 states that there is a maximum of six critical points and a minimum of two critical points. There are two pairs of free critical points conjugate to each other, each with the same characteristics in terms of stability, simplifying the dynamical analysis.

Parameter values that reduce the number of free critical points are interesting for drawing dynamical planes.

3.5. Parameter Spaces. The dynamical behavior of operator $R_\theta(x)$ depends on the values of parameter θ. Parameter spaces are graphs of the independent-free critical values for the method, which allow to visualize parameter values that make the method stable or unstable [13].

We generate the parameter spaces, taking a free critical point $\mathrm{cl}(\theta)$ as initial estimation for operator $R_\theta(x)$ and applying the iterative scheme (4) for all values of the parameter θ, defined on a mesh of the complex plane with 800 points on each axis. These plots have been generated using

MATLAB R2020b. At a point corresponding to a specific value of θ, if a method converges to one of the roots of the polynomial in less than 200 iterations and with an error estimate of less than 10^{-3}, then that point is colored red; otherwise, the point is colored black.

The Jarratt parametric family has at most four free critical points, of which there are two pairs conjugate to each other (see Proposition 7); that means there are only two independent free critical points. We then obtain two different parameter spaces: P_1 for $x = \mathrm{cl}_1(\theta), \mathrm{cl}_2(\theta)$ and P_2 for $x = \mathrm{cl}_3(\theta), \mathrm{cl}_4(\theta)$, shown in Figure 4.

In P_1 parameter space (Figure 4(a)), the all-red surface means that for any method of the family, in that range of θ values, the critical point $\mathrm{cl}_1(\theta)$ is only able to converge to one of the two roots of the polynomial. This critical point does not create its own basin; there is no attracting strange free point and no attracting periodic orbit, the only attractors are the roots of the polynomial themselves. The critical point $\mathrm{cl}_2(\theta)$ has the same behavior as $\mathrm{cl}_1(\theta)$, being both conjugate to each other.

In the parameter plane P_2 corresponding to the conjugate critical points $\mathrm{cl}_3(\theta)$ and $\mathrm{cl}_4(\theta)$, the region marked in red corresponds to points where the method has stable behavior, while the regions in black correspond to points where the method has unstable behavior. Regions where strange fixed points are attractors and are also unstable and appear in this parameter space (see Figure 4(b)).

3.6. Dynamical Planes. To study the stability of some methods for Jarratt parametric family, we use dynamical planes. These plots allow us to extend the information obtained in the parameter planes; in them, we can visualize the basins of attraction for fixed or periodic points of the method, given some particular value of parameter, θ [13].

For the dynamical analysis we select methods of family (4) corresponding to parameter values located in the stability zone and in the instability zone of the parameter space, and from these we will generate the corresponding dynamical planes, using MATLAB R2020b. In these figures, a mesh with 800 points on each axis has been drawn, where each point represents a different initial estimate that is introduced in the iterative process (see [13]). When a method converges to a solution, in at most 200 iterations and with a tolerance of less than 10^{-3}, then, it is assigned a certain color: orange if it converges to $x = 0$ and blue if it converges to $x = \infty$. In case the initial estimate does not converge to any of the roots of the polynomial within the maximum number of iterations, it is assigned the color black; other basins of attraction are colored green and red.

Figure 5 shows dynamical planes for values of θ in the stability zone, in which only two basins of attraction corresponding to the roots are observed. Specifically, some methods appear with global convergence, which is a key fact in some applications, such as the finding of matrix sign functions by using these iterative methods (see, for example, [14, 15]).

Figure 6 shows dynamical planes for values of θ outside the stability zone, which can be visually verified by the existence of black areas of nonconvergence to the solution (in the case of Figures 6(a) and 6(b)) and by the presence of two basins of attraction that do not correspond to roots, but to conjugate strange fixed points (in the case of Figures 6(c) and 6(d)).

4. Numerical Results

The numerical tests in this section have been performed using variable precision arithmetic, with 2000 digits of mantissa and a tolerance of 10^{-100} in MATLAB R2020b. The stopping criterion used is $|x_{k+1} - x_k| < 10^{-100}$ or $|f(x_{k+1})| < 10^{-100}$.

Tables 1–3 summarize the results obtained by applying four different methods of the family, some of them stable ($FJ2(\theta = 1.5)$ and $FJ3(\theta = 2.75)$) and others unstable ($FJ1(\theta = -0.4)$ and $FJ4(\theta = 3)$), as well as the methods of Chun [16] and Ostrowski [17], which have order of convergence four. The test functions used are the following:

(i) $f_1(x) = e^x - 4x^2$, $\alpha \approx 0.714806$

(ii) $f_2(x) = \cos(x) - x$, $\alpha \approx 0.739085$

(iii) $f_3(x) = e^x - 1.5 - \arctan(x)$, $\alpha \approx 0.767653$

(iv) $f_4(x) = \sin(x) - x^2 + 1$, $\alpha \approx 1.409624$.

In order to evaluate the stringency of each implemented method with respect to the initial estimate to find a solution, we have started the iterations with different initial estimates, named according to their proximity to the solution x_0: close ($x_0 \approx \alpha$), far ($x_0 \approx 10\alpha$), and very far ($x_0 \approx 100\alpha$), respectively.

For each function, the following items have been calculated: approximate root value, error estimates at the last iteration: $|x_{k+1} - x_k|$ and $|f(x_{k+1})|$, the number of iterations required to converge to the solution, the approximate computational convergence order (ACOC), and the elapsed time (e-time), calculated as the arithmetic mean of 10 runs for each method.

Table 1 shows that when the initial estimate is close to the root, the presented methods converge, for a minimum of 5 iterations and a maximum of 6 iterations, even in cases of those corresponding to parameter values for family (4) located in regions of instability.

It can also be observed that the lowest error corresponds to Chun's method, followed by the stable $FJ3$ method. The number of iterations is in general the same and the order of computational convergence obtained for all methods of the family confirms the theoretical convergence order determined in Section 2

From Tables 2 and 3, we can observe that the presented methods do not always converge to the solution, supporting the results found in the dynamical analysis of Section 3. The convergence depends on the initial estimation and the nonlinear function used.

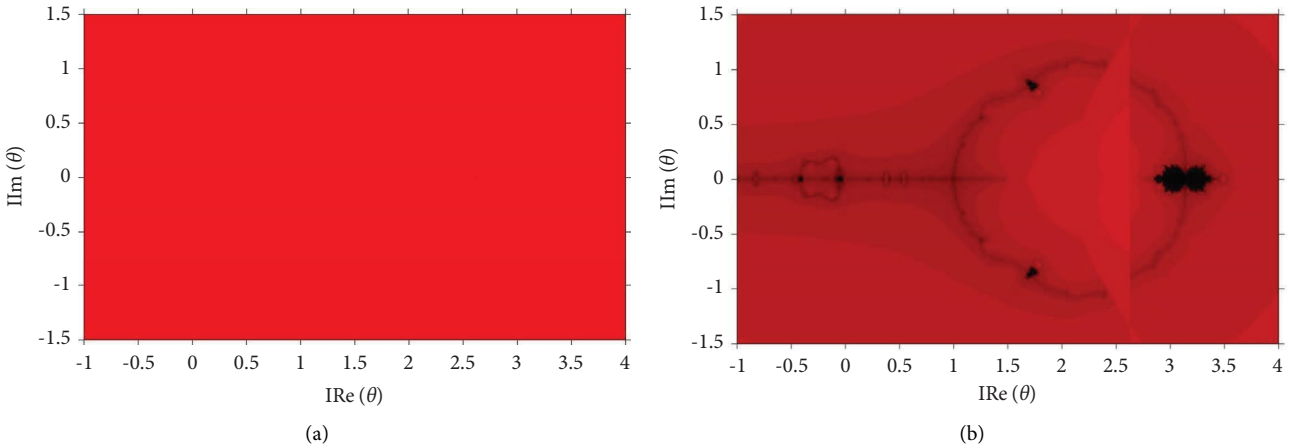

FIGURE 4: Parameter spaces of the free critical points (in red color, the complex area corresponding to the stability region). (a) P_1 for $x = \mathrm{cl}_1(\theta), \mathrm{cl}_2(\theta)$. (b) P_2 for $x = \mathrm{cl}_3(\theta), \mathrm{cl}_4(\theta)$.

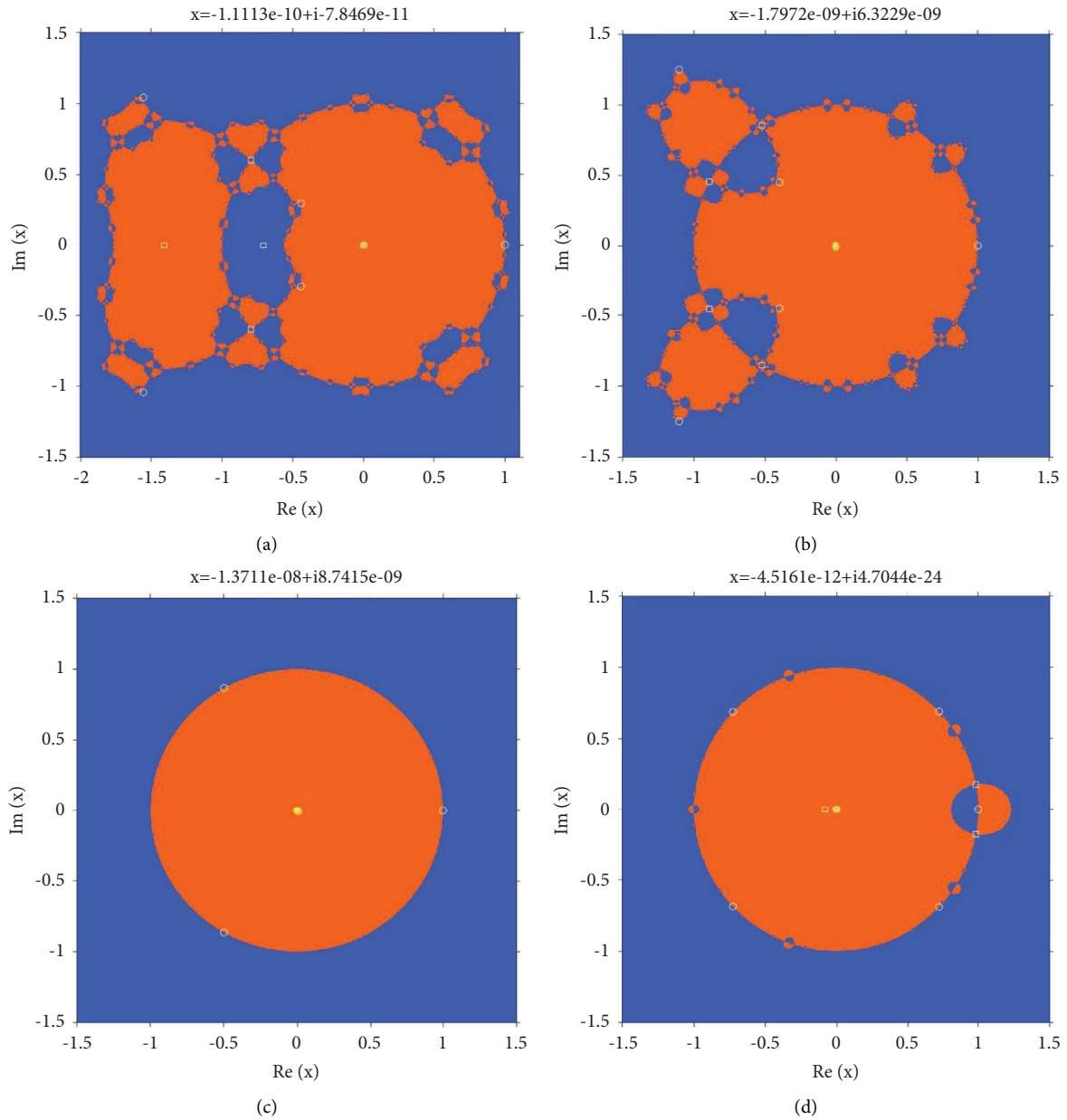

FIGURE 5: Dynamical planes for methods within the stability region (orange color corresponds to the 0 basin of attraction, blue color to the ∞ basin). (a) $\theta = -0.25$. (b) $\theta = 0.5$. (c) $\theta = 1.5$. (d) $\theta = 2.75$.

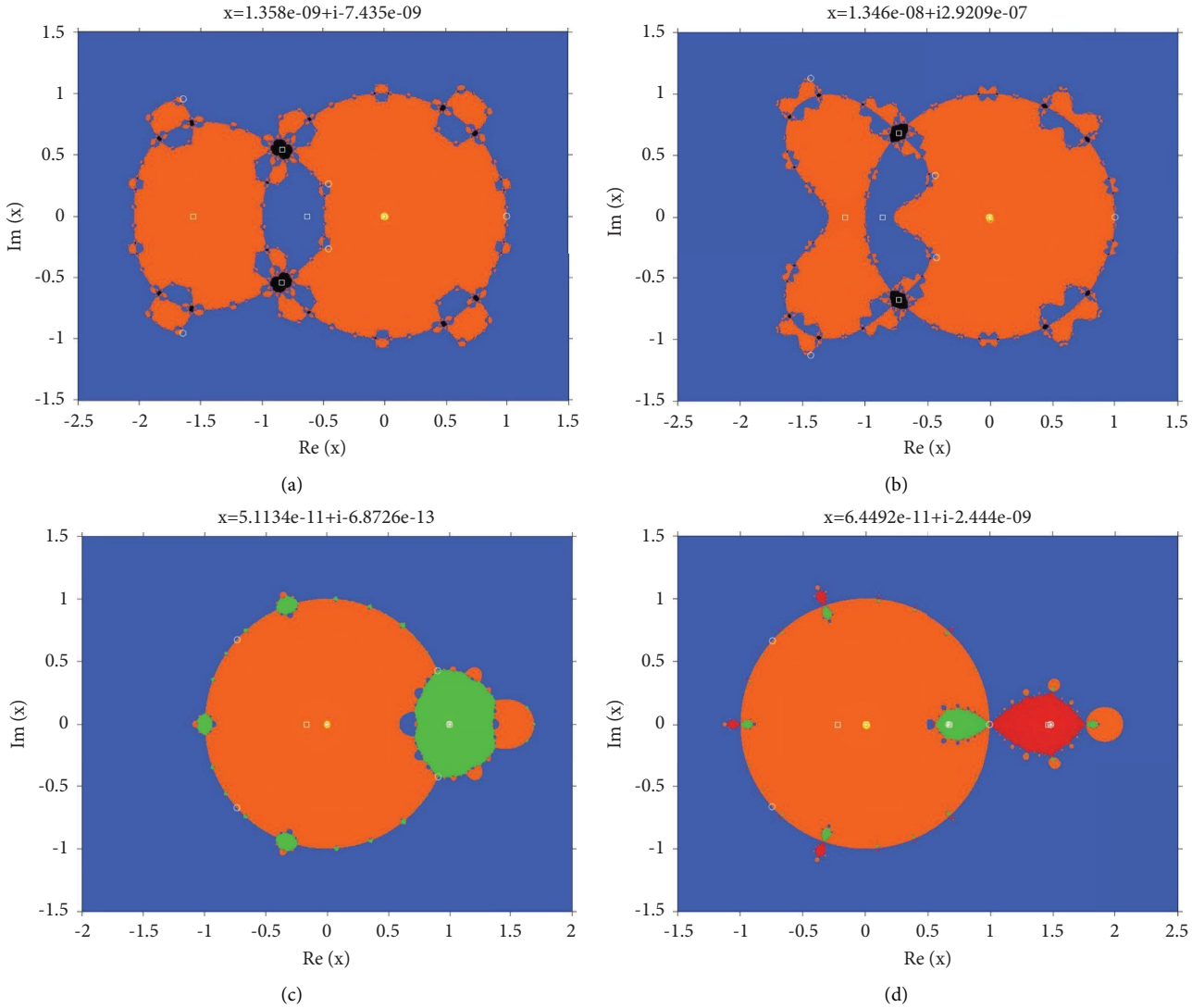

Figure 6: Dynamical planes for methods outside the stability region (orange color corresponds to the 0 basin of attraction, blue color to the ∞ basin, and green and red colors correspond to basins of attraction of conjugate strange fixed points). (a) $\theta = -0.40$. (b) $\theta = -0.05$. (c) $\theta = 3$. (d) $\theta = 3.25$.

Table 1: Numerical performance of iterative methods in nonlinear equations for x_0 close to α.

Function	Method	α	$\lvert x_{k+1} - x_k \rvert$	$\lvert f(x_{k+1} - x_k) \rvert$	Iter	ACOC	e-time
f_1 $x_0 = 0.6$	$FJ1_{\theta=-0.4}$	0.714806	2.946×10^{-207}	1.0823×10^{-206}	5	4.00	0.20
	$FJ2_{\theta=1.5}$	0.714806	9.1492×10^{-248}	3.362×10^{-247}	5	4.00	0.20
	$FJ3_{\theta=2.75}$	0.714806	2.3560×10^{-347}	8.6576×10^{-347}	5	4.00	0.19
	$FJ4_{\theta=3.0}$	0.714806	1.1911×10^{-345}	4.3769×10^{-345}	5	4.00	0.10
	Ostrowski	0.714806	1.2227×10^{-247}	4.4928×10^{-247}	5	4.00	0.18
	Chun	0.714806	2.5054×10^{-181}	9.2064×10^{-181}	5	4.00	0.15
f_2 $x_0 = 0.5$	$FJ1_{\theta=-0.4}$	0.739085	3.1924×10^{-261}	5.3428×10^{-261}	5	4.00	0.15
	$FJ2_{\theta=1.5}$	0.739085	1.3808×10^{-288}	2.311×10^{-288}	5	4.00	0.13
	$FJ3_{\theta=2.75}$	0.739085	3.0484×10^{-321}	5.1037×10^{-321}	5	4.00	0.16
	$FJ4_{\theta=3.0}$	0.739085	2.0635×10^{-332}	3.4534×10^{-332}	5	4.00	0.21
	Ostrowski	0.739085	8.6024×10^{-286}	1.4397×10^{-285}	5	4.00	0.15
	Chun	0.739085	1.5559×10^{-239}	2.6039×10^{-239}	5	4.00	0.18
f_3 $x_0 = 1$	$FJ1_{\theta=-0.4}$	0.767653	2.3863×10^{-165}	3.6403×10^{-165}	5	4.00	0.25
	$FJ2_{\theta=1.5}$	0.767653	4.2565×10^{-200}	6.4932×10^{-200}	5	4.00	0.23
	$FJ3_{\theta=2.75}$	0.767653	5.7081×10^{-209}	8.7077×10^{-209}	5	4.00	0.17
	$FJ4_{\theta=3.0}$	0.767653	2.0361×10^{-190}	3.1061×10^{-190}	5	4.00	0.16
	Ostrowski	0.767653	1.6357×10^{-200}	2.4953×10^{-200}	5	4.00	0.17
	Chun	0.739085	6.6244×10^{-146}	1.0105×10^{-145}	5	4.00	0.18
f_4 $x_0 = 1.1$	$FJ1_{\theta=-0.4}$	1.409624	1.0809×10^{-124}	2.8739×10^{-124}	5	4.00	0.16
	$FJ2_{\theta=1.5}$	1.409624	3.5952×10^{-177}	9.5588×10^{-177}	5	4.00	0.14
	$FJ3_{\theta=2.75}$	1.409624	1.739×10^{-268}	4.6237×10^{-268}	5	4.00	0.16
	$FJ4_{\theta=3.0}$	1.409624	1.3974×10^{-261}	3.7153×10^{-261}	5	4.00	0.16
	Ostrowski	1.409624	6.8618×10^{-177}	1.8244×10^{-176}	5	4.00	0.16
	Chun	1.409624	1.5326×10^{-377}	4.0750×10^{-377}	6	4.00	0.18

Table 2: Numerical performance of iterative methods in nonlinear equations for x_0 far from α.

Function	Method	α	$\lvert x_{k+1} - x_k \rvert$	$\lvert f(x_{k+1} - x_k) \rvert$	Iter	ACOC	e-time
f_1 $x_0 = 6$	$FJ1_{\theta=-0.4}$	4.306585	5.8656×10^{-107}	0	6	4.00	0.21
	$FJ2_{\theta=1.5}$	4.306585	0	0	6	4.00	0.13
	$FJ3_{\theta=2.75}$	5.285458	5.4014×10^{-01}	2.0311×10^{02}	50	0.94	0.47
	$FJ4_{\theta=3.0}$	4.306585	$7,1981 \times 10^{-130}$	2.8601×10^{-128}	8	4.00	0.23
	Ostrowski	4.306585	0	0	6	4.00	0.13
	Chun	4.306585	0	0	7	4.00	0.14
f_2 $x_0 = 5$	$FJ1_{\theta=-0.4}$	-2.8254×10^{19}	3.3407×10^{19}	6.1661×10^{19}	50	0.51	0.62
	$FJ2_{\theta=1.5}$	-1.9303×10^{11}	$2.7694 \times 10^{+11}$	$4.6998 \times 10^{+11}$	50	−0.78	0.38
	$FJ3_{\theta=2.7}$	0.739085	8.8637×10^{-368}	1.4835×10^{-368}	10	4.00	0.17
	$FJ4_{\theta=3.0}$	0.739085	4.9476×10^{-209}	8.2804×10^{-209}	10	4.00	0.29
	Ostrowski	0.739085	1.6478×10^{-376}	2.7579×10^{-376}	8	4.00	0.15
	Chun	3.8427×10^{02}	1.4659×10^{05}	1.4620×10^{05}	50	0.91	0.34
f_3 $x_0 = 10$	$FJ1_{\theta=-0.4}$	0.767653	7.7401×10^{-375}	1.1807×10^{-374}	11	4.00	0.27
	$FJ2_{\theta=1.5}$	0.767653	0	0	9	4.00	0.16
	$FJ3_{\theta=2.75}$	5.249817	1.1877	6.2192×10^{02}	50	−0.54	0.55
	$FJ4_{\theta=3.0}$	−14.101270	0	0	13	4.00	0.21
	Ostrowski	0.767653	0	6.045×10^{-141}	9	4.00	0.17
	Chun	0.767653	0	0	11	4.00	0.17
f_4 $x_0 = 11$	$FJ1_{\theta=-0.4}$	1.409624	5.6762×10^{-289}	1.5092×10^{-288}	7	4.00	0.16
	$FJ2_{\theta=1.5}$	1.409624	0	0	6	4.00	0.12
	$FJ3_{\theta=2.75}$	1.409624	0	0	7	4.00	0.15
	$FJ4_{\theta=3.0}$	1.409624	0	0	8	4.00	0.22
	Ostrowski	1.409624	1.2412×10^{-364}	2.7166×10^{-369}	7	4.00	0.13
	Chun	1.409624	2.1129×10^{-192}	5.6178×10^{-192}	7	4.00	0.12

Table 3: Numerical performance of iterative methods in nonlinear equations for x_0 very far from α.

Function	Method	α	$\lvert x_{k+1} - x_k \rvert$	$\lvert f(x_{k+1} - x_k) \rvert$	Iter	ACOC	e-time
f_1 $x_0 = 60$	$FJ1_{\theta=-0.4}$	4.306585	1.0880×10^{-295}	0	36	4.00	0.42
	$FJ2_{\theta=1.5}$	4.306585	0	0	29	4.00	0.29
	$FJ3_{\theta=2.75}$	6.111780	0.9371	9.5286×10^{02}	50	0.14	0.48
	$FJ4_{\theta=3.0}$	4.952518	0.6576	1.472906×10^{02}	50	2.45	0.71
	Ostrowski	4.306585	0	0	29	4.00	0.277
	Chun	4.306585	0	0	40	4.00	0.32
f_2 $x_0 = 50$	$FJ1_{\theta=-0.4}$	-4.1306×10^{31}	3.3587×10^{31}	7.7189×10^{30}	50	0.81	0.52
	$FJ2_{\theta=1.5}$	-7.7013×10^{04}	7.7992×10^{04}	1.5501×10^{05}	50	−0.39	0.43
	$FJ3_{\theta=2.7}$	0.739085	6.9742×10^{-290}	1.1672×10^{-289}	18	4.00	0.21
	$FJ4_{\theta=3.0}$	-2.4795×10^{22}	4.9602×10^{22}	2.4807×10^{22}	50	−0.10	0.46
	Ostrowski	0.739085	9.2752×10^{-229}	0	8	4.00	0.12
	Chun	0.739085	1.8401×10^{-337}	3.0796×10^{-337}	8	4.00	0.12
f_3 $x_0 = 100$	$FJ1_{\theta=-0.4}$	7.223356	1.8545	8.7563×10^{03}	50	6.34	0.50
	$FJ2_{\theta=1.5}$	0.767653	4.2443×10^{-445}	6.4746×10^{-245}	48	4.00	0.49
	$FJ3_{\theta=2.75}$	40.033796	1.1993	8.0782×10^{17}	50	3.32	0.54
	$FJ4_{\theta=3.0}$	33.267173	1.3347	1.0651×10^{15}	50	3.80	0.52
	Ostrowski	0.767653	0	0	47	4.00	0.40
	Chun	18.0725	1.6385	3.6341×10^{08}	50	5.14	0.44
f_4 $x_0 = 110$	$FJ1_{\theta=-0.4}$	1.409624	3.2545×10^{-378}	8.6531×10^{-378}	9	4.00	0.20
	$FJ2_{\theta=1.5}$	1.409624	0	4.9630×10^{-155}	8	4.00	0.15
	$FJ3_{\theta=2.75}$	−0.636733	0	5.8261×10^{-127}	10	4.00	0.17
	$FJ4_{\theta=3.0}$	NaN	NaN	NaN	12	NaN	0.36
	Ostrowski	1.409624	0	0	4	4.00	0.13
	Chun	1.409624	1.9130×10^{-194}	5.0862×10^{-194}	9	4.00	0.15

When the initial estimate is far or very far from the root, in general, the $FJ1(\theta = -0.4)$ and $FJ4(\theta = 3.0)$ methods diverge, as expected, since these methods correspond to parameter values located in the instability zone.

5. Conclusions

In this paper, the dynamical study of a family of fourth-order iterative methods has been carried out in order to identify those members of the family that have a better behavior in terms of stability.

The dynamical behavior of the Jarratt parametric family is generally stable. This is shown in the parameter spaces, where the prevalence of the stability regions is observed, and it is confirmed by numerical tests, which yield favorable results on the convergence of the studied methods. The theoretical order of convergence has been confirmed by ACOC, which is approximately equal to 4.

For initial estimates close to the solution, all methods converge. Divergence cases are verified for initial estimates far or very far from the solution, especially for methods of the considered family located in the instability zone.

Therefore, we conclude after the analytic, dynamic, and numerical studies performed in this manuscript, that classical Jarratt's scheme is the best one among all the general class of iterative methods proposed originally by Jarratt. In future work, we will extend this scheme to the estimation of matrix sign functions and other nonlinear matrix equations.

Data Availability

No underlying data were collected or produced in this study.

Conflicts of Interest

The authors declare that they have no conflicts of interest.

Acknowledgments

The authors acknowledge the open access funding enabled and organized by CRUE-UNIRIS Gold.

References

[1] S. Regmi, *Optimized Iterative Methods with Applications in Diverse Disciplines*, Nove Science Publisher, New York, NY, USA, 2021.

[2] M. Petkovic, B. Neta, L. Petkovic, and J. Dzunic, *Multipoint Methods for Solving Nonlinear Equations*, Elsevier, Amsterdam, Netherlands, 2013.

[3] S. Amat and S. Busquier, *Advances in Iterative Methods for Nonlinear Equations*, SEMA-SEMAI Springer series, Switzerland, 2016.

[4] A. Cordero, M. Moscoso-Martínez, and J. R. Torregrosa, "Chaos and stability in a new iterative family for solving nonlinear equations," *Algorithms*, vol. 14, no. 4, p. 101, 2021.

[5] A. Cordero, J. García-Maimó, J. R. Torregrosa, M. P. Vassileva, and P. Vindel, "Chaos in King's iterative family," *Applied Mathematics Letters*, vol. 26, no. 8, pp. 842–848, 2013.

[6] J. García, *Análisis dinámico y numérico de las familias de métodos iterativos para la resolución de ecuaciones no lineales y su extensión a espacios de Banach*, Universitat Politècnica de València, Valencia, Spain, Ph.D, 2017.

[7] P. Jarratt, "Some fourth order multipoint iterative methods for solving equations," *Mathematics of Computation*, vol. 20, no. 95, pp. 434–437, 1966.

[8] F. I. Chicharro, *Análisis dinámico y aplicaciones de métodos iterativos de resolución ecuaciones no lineales*, Universitat Politècnica de València, Valencia, Spain, Ph.D, 2017.
[9] R. L. Devaney, *An Introduction to Chaotic Dynamical Systems*, Chapman & Hall, 2022.
[10] H. T. Kung and J. F. Traub, "Optimal order of one-point and multipoint iteration," *Journal of the ACM*, vol. 21, no. 4, pp. 643–651, 1974.
[11] P. Fatou, "Sur les 'equations fonctionelles," *Bulletin de la Société Mathématique de France*, vol. 47, pp. 161–271, 1919.
[12] G. Julia, "Memoire sur l'iteration des fonctions rationnelles," *Journal de Mathematiques Pures et Appliquees*, vol. 8, pp. 47–245, 1918.
[13] A. Cordero and J. R. Torregrosa, *On the Design for Optimal Iterative Methods for Solving Nonlinear Equations. Book: Advances in Iterative Methods for Nonlinear Equations*, Springer, Berlin, Germany, 2016.
[14] A. Cordero, F. Soleymani, J. R. Torregrosa, and M. Z. Ullah, "Numerically stable improved Chebyshev–Halley type schemes for matrix sign function," *Journal of Computational and Applied Mathematics*, vol. 318, pp. 189–198, 2017.
[15] A. R. Soheili, F. Toutounian, and F. Soleymani, "A fast convergent numerical method for matrix sign function with application in SDEs," *Journal of Computational and Applied Mathematics*, vol. 282, pp. 167–178, 2015.
[16] C. Chun, "Some fourth-order iterative methods for solving nonlinear equations," *Applied Mathematics and Computation*, vol. 195, no. 2, pp. 454–459, 2008.
[17] A. M. Ostrowski, *Solutions of Equations and System of Equations*, Academic Press, New York, NY, USA, 1960.